ISSN 1560-3547, Regular and Chaotic Dynamics, 2019, Vol. 24, No. 6, pp. 725–738. © Pleiades Publishing, Ltd., 2019.

Topaj – Pikovsky Involution in Hamiltonian Lattice of Locally Coupled Oscillators

Vyacheslav P. Kruglov[1, 2, 3*] and Sergey P. Kuznetsov[1, 2]**

[1] *Udmurt State University*
ul. Universitetskaya 1, Izhevsk, 426034 Russia

[2] *Kotelnikov's Institute of Radio-Engineering and Electronics of RAS, Saratov Branch*
ul. Zelenaya 38, Saratov, 410019 Russia

[3] *Steklov Mathematical Institute, Russian Academy of Sciences*
ul. Gubkina 8, Moscow, 119991 Russia

Received October 28, 2019; revised November 01, 2019; accepted November 11, 2019

Abstract—We discuss Hamiltonian model of oscillator lattice with local coupling. The Hamiltonian model describes localized spatial modes of nonlinear Schrödinger equation with periodic tilted potential. The Hamiltonian system manifests reversibility of Topaj – Pikovsky phase oscillator lattice. Furthermore, the Hamiltonian system has invariant manifolds with asymptotic dynamics exactly equivalent to the Topaj – Pikovsky model. We examine the stability of trajectories belonging to invariant manifolds by means of numerical evaluation of Lyapunov exponents. We show that there is no contradiction between asymptotic dynamics on invariant manifolds and conservation of phase volume of Hamiltonian system. We demonstrate the complexity of dynamics with results of numerical simulations.

MSC2010 numbers: 37J15, 37C10, 37C70, 34D08, 34C15, 34C60

DOI: 10.1134/S1560354719060108

Keywords: reversibility, involution, Hamiltonian system, Topaj – Pikovsky model, phase oscillator lattice

1. INTRODUCTION

Lattices of phase oscillators compel attention of researchers for many years [1, 2, 4]. Each oscillator in a lattice is described by a single cyclic variable and governed by first order differential equation. Usually phase oscillators are derived from second order dissipative systems with a stable limit cycle, like van der Pol oscillators, by neglecting the amplitude variations. Then the phase is a slow variable that parametrizes the limit cycle. Phase oscillators also describe dissipative pendulums or Josephson junctions at overdumped limit. The lattices of phase oscillators share with lattices of second order dissipative oscillators a feature of synchronous regimes, but interestingly also manifest behaviour unexpected in dissipative systems. There are examples of phase oscillator lattices that demonstrate reversibility. A well-known example of reversible lattice was given by Pikovsky and Topaj [5]. This model is rigorously studied [6, 7] and is of great interest to us. Reversibility was noticed also in an array of overdumped Josephson junctions shunted by resistive load [8]. Tsang et al. [8] had found the time-reversing change of variables and emphasized that in-phase state in such array was not an attractor. They also pointed out that time reversal symmetry had vanished upon introduction of second derivatives (if junction capacities are non-negligible or resistance load is replaced by LC-load). Before we proceed with the discussion of Topaj – Pikovsky lattice, we outline shortly a range of related issues.

A dynamical system is called reversible if there is a change of variables $\mathbf{R}$ which if combined with time reversal $t \mapsto -t$ leaves equations invariant [9–12]. Such transformation most often is an involution which means that it yields the identity when composed with itself: $\mathbf{R} \circ \mathbf{R} = Id$.

*E-mail: kruglovyacheslav@gmail.com
**E-mail: spkuz@yandex.ru

Involution $\mathbf{R}$ has a fixed set Fix$\mathbf{R}$, and trajectories that intersect it are called symmetric [11]. While time-reversal symmetry occurs naturally in Hamiltonian dynamical systems, the definition of reversible system is not bounded just to this class [9, 10]. Generally a reversible dynamical system has "conservative" symmetric trajectories (with zero sum of Lyapunov exponents) and pairs of attractors and repellers that map into each other under involution and are connected by symmetric asymptotic trajectories. Behaviour of "conservative" trajectories resembles Hamiltonian systems, there is a variant of KAM-theorem for reversible systems [13–15]. The dynamics of reversible systems is classified differently from both conservative and dissipative and is referred as "mixed" in recent articles [12, 16, 17]. There are well known physical examples of reversible but not Hamiltonian systems. Reversible dynamics manifests in CO_2 lasers [18], point vortices interacting with potential wave [19–21], mechanical systems with nonholonomic constraints [22–27]. There is a lot of work done recently regarding Hamiltonization of nonholonomic systems [28–32].

Pikovsky and Topaj [5] considered a relatively simple chain of N locally coupled phase oscillators with linear distrubution of natural frequencies, which has time reversal symmetry:

$$\dot{\phi}_j = \omega_j + \varepsilon \sin\left(\phi_{j+1} - \phi_j\right) + \varepsilon \sin\left(\phi_{j-1} - \phi_j\right), \tag{1.1}$$

where ϕ_j are phases of oscillators, chain boundaries are ϕ_1 and ϕ_N, ω_j are natural frequencies, which are equidistant: $\omega_{j+1} - \omega_j = 1$. Oscillators are coupled via $\sin\psi_j$, where ψ_j are phase shifts $\phi_{j+1} - \phi_j$. Boundary conditions are free: $\phi_0 = \phi_1$ and $\phi_{N+1} = \phi_N$. Since right-hand-sides depend only on phase shifts ψ_j, one can easily derive a system of $N - 1$ equations:

$$\dot{\psi}_j = 1 + \varepsilon \sin\psi_{j+1} + \varepsilon \sin\psi_{j-1} - 2\varepsilon \sin\psi_j. \tag{1.2}$$

For Eq. (1.2) involution is

$$\mathbf{R} : \psi_j \mapsto \pi - \psi_{N-j}. \tag{1.3}$$

Involution (1.3) has an invariant set Fix$\mathbf{R} : \psi_j + \psi_{N-j} = \pi$.

Pikovsky and Topaj observed numerically an almost conservative behaviour of system (1.2) at small values of coupling ε and attractors and repellers, corresponding to phase-locked clusters of oscillators, at large values of ε. Gonchenko et al. [6] described bifurcations leading to the emergence of attractors and repellers within "conservative chaotic sea".

The aim of this work is to observe the phenomenon of reversibility in more general lattices of oscillators. Since it is clear that reversibility is hard to expect with second order dissipative oscillators, we apply a model with energy conserved. Actually we use a Hamiltonian model of coupled oscillators, introduced in [33] and discussed in [34]. This Hamiltonian model has an involution very close to Topaj – Pikovsky model and invariant manifolds, on which amplitudes are constant and phases are governed exactly by Topaj – Pikovsky equations. We should emphasize however, that these invariant manifolds are not asymptotically stable in contrast to phase dynamics of lattices of non-conservative oscillators.

2. MODEL OF HAMILTONIAN LATTICE

Tommen et al. [33] studied numerically the classical limit model of an ultracold quantum degenerate gas in a tilted optical lattice. They derived Hamiltonian equations governing complex amplitudes z_j of nonlinear Schrödinger equation with tilted potential:

$$i\partial_t\psi = -\frac{\hbar^2}{2m}\partial_{xx}\psi + \left(V_0\cos^2 kx + Fx\right)\psi + g|\psi|^2\psi. \tag{2.1}$$

Assuming that potential wells are deep, such that only ground states are excited, one can substitute the anzatz $\psi\left(x,t\right) = \sum_{j=1}^{N} z_j\left(t\right)\Psi_j\left(x\right)$ in Eq. (2.1). Here N is the number of potential wells, $\Psi_j\left(x\right)$ are Wannier – Stark states (the resonant eigenstates of linear Schrödinger equation) localized in potential wells, and $z_j(t)$ describe oscillations in potential wells. This expansion yields equations of motion (we suggest to find full derivation in [33–35])

$$\begin{aligned}\dot{z}_j =& i\frac{\partial\mathcal{H}}{\partial\bar{z}_j} = i\omega_j z_j + i\beta|z_j|^2 z_j\\ &+ \varepsilon\left(2|z_j|^2\left(z_{j+1}+z_{j-1}\right) - z_j^2\left(\bar{z}_{j+1}+\bar{z}_{j-1}\right) - |z_{j+1}|^2 z_{j+1} - |z_{j-1}|^2 z_{j-1}\right),\\ \dot{\bar{z}}_j =& -i\frac{\partial\mathcal{H}}{\partial z_j} = -i\omega_j\bar{z}_j - i\beta|z_j|^2\bar{z}_j\\ &+ \varepsilon\left(2|z_j|^2\left(\bar{z}_{j+1}+\bar{z}_{j-1}\right) - \bar{z}_j^2\left(z_{j+1}+z_{j-1}\right) - |z_{j+1}|^2\bar{z}_{j+1} - |z_{j-1}|^2\bar{z}_{j-1}\right),\end{aligned} \tag{2.2}$$

which are generated by Hamiltonian

$$\mathcal{H}\left(\ldots,z_j,\bar{z}_j,\ldots\right) = \sum_{j=1}^{N}\omega_j z_j\bar{z}_j + \frac{1}{2}\beta\sum_{j=1}^{N} z_j^2\bar{z}_j^2 + i\varepsilon\sum_{j=1}^{N}\left(z_{j+1}\bar{z}_{j+1} - z_j\bar{z}_j\right)\left(z_{j+1}\bar{z}_j - z_j\bar{z}_{j+1}\right), \tag{2.3}$$

where ε is coupling parameter and ω_j are natural frequencies of oscillations in potential wells. Only local interaction is assumed in Eq. (2.2) since Wannier – Stark states are localized. The frequencies in Eq. (2.2) are equidistant: $\omega_j = -\frac{\pi F}{k\hbar}j$ (we will use $\omega_{j+1}-\omega_j = 1$ onwards). The boundary conditions are $z_0 = z_1$, $z_{N+1} = z_N$. It is important to our purposes to rewrite Hamiltonian (2.3) with different set of canonical variables $I_j = |z_j|^2$ (the populations of potential wells or intensities of oscillations) and $\phi_j = \mathrm{Arg} z_j$ (phases of oscillations):

$$\mathcal{H}\left(\ldots,I_j,\phi_j,\ldots\right) = \sum_{j=1}^{N}\omega_j I_j + \frac{1}{2}\beta\sum_{j=1}^{N} I_j^2 - 2\varepsilon\sum_{j=1}^{N}\sqrt{I_{j+1}I_j}\left(I_{j+1}-I_j\right)\sin\left(\phi_{j+1}-\phi_j\right). \tag{2.4}$$

Hamiltonian function (2.4) produces $2N$ dynamical equations

$$\begin{aligned}\dot{I}_j =& -\frac{\partial\mathcal{H}}{\partial\phi_j} = -2\varepsilon\sqrt{I_{j+1}I_j}\left(I_{j+1}-I_j\right)\cos\left(\phi_{j+1}-\phi_j\right)\\ &\qquad - 2\varepsilon\sqrt{I_{j-1}I_j}\left(I_{j-1}-I_j\right)\cos\left(\phi_{j-1}-\phi_j\right),\\ \dot{\phi}_j =& \frac{\partial\mathcal{H}}{\partial I_j} = \omega_j + \beta I_j + \varepsilon\left\{3\sqrt{I_{j+1}I_j} - I_{j+1}\sqrt{\frac{I_{j+1}}{I_j}}\right\}\sin\left(\phi_{j+1}-\phi_j\right)\\ &\qquad + \varepsilon\left\{3\sqrt{I_{j-1}I_j} - I_{j-1}\sqrt{\frac{I_{j-1}}{I_j}}\right\}\sin\left(\phi_{j-1}-\phi_j\right),\end{aligned} \tag{2.5}$$

with free boundary conditions $\phi_0 = \phi_1$, $\phi_{N+1} = \phi_N$, $I_0 = I_1$, $I_{N+1} = I_N$.

Witthaut and Timme introduced equations [34] similar to Eq. (2.5) but with global coupling of oscillators. They pointed out that phase space of the Hamiltonian model includes invariant manifolds with dynamics exactly matching Kuramoto model [1, 2, 4]. We however restrict ourselves to the case of local coupling also covered in [34].

If populations of all oscillators are equal to each other, $I_j = I$, they are constant, $\dot{I}_j = 0$. Therefore an infinite family of invariant N-dimensional tori exists with constant equal populations I of oscillators and phases ϕ_j governed by only N equations

$$\dot{\phi}_j = \omega_j + \beta I + 2\varepsilon I\sin\left(\phi_{j+1}-\phi_j\right) + 2\varepsilon I\sin\left(\phi_{j-1}-\phi_j\right). \tag{2.6}$$

This is just the Eq. (1.1) with rescaled coupling $2\varepsilon I$ and shifted frequencies $\omega_j + \beta I$. Thus, on every invariant torus $I_j = I$ the Hamiltonian function (2.4) generates a system of phase oscillators with local coupling. As before, one can change phases ϕ_j to phase shifts $\psi_j = \phi_{j+1} - \phi_j$ and reduce the phase space dimension of phase model (2.6) or Hamiltonian model (2.5) by one.

It is not surprising that Hamiltonian model (2.5) is reversible with involution just slightly more comlpicated[1)]:

$$\mathbf{R}: I_j \mapsto I_{N-j+1},\ (\phi_{j+1}-\phi_j) \mapsto \pi - (\phi_{N-j+1}-\phi_{N-j}). \tag{2.7}$$

Involution (2.7) has an invariant set Fix$\mathbf{R}$: $I_j - I_{N-j+1} = 0,\ (\phi_{j+1}-\phi_j) + (\phi_{N-j+1}-\phi_{N-j}) = \pi$. One can rewrite transformation (2.7) in complex variables $z_j = \sqrt{I_j}e^{i\phi_j}$:

$$\mathbf{R}': z_j \mapsto \bar{z}_{N-j+1},\ \omega_j \mapsto \omega_{N-j+1}. \tag{2.8}$$

This transform can be considered as a composition of the flip of the lattice relative to its central part ($j \mapsto N-j+1$) and complex conjugation of all amplitudes $z_j \mapsto \bar{z}_j$. A trajectory symmetric by $\mathbf{R}'$ corresponds physically to the case of lattice elements positioned symmetrically relative to the center and rotating in opposite directions. The requirement of frequencies flip $\omega_j \mapsto \omega_{N-j+1}$ is important. However since $\omega_{j+1} - \omega_j = 1$, transformation $\mathbf{R}$ (2.7) does not explicitly include the change of parameters.

System (2.5) has two constants of motion [34]. One of them is the Hamiltonian function $\mathcal{H}$, another is the total population of oscillators (sum of intensities):

$$C^2 = \sum_{j=1}^{N} I_j = \sum_{j=1}^{N} z_j \bar{z}_j. \tag{2.9}$$

C^2 is constant due to norm preservation of nonlinear Schrödinger equation (2.1). It makes the dynamics equivariant under a simultaneous scaling $I_j \mapsto C^2 I_j$ (or $z_j \mapsto C z_j$) and parameter transformation $\varepsilon \mapsto \varepsilon/C^2$, $\beta \mapsto \beta/C^2$ for all j and any $C > 0$ [34]. This scaling does not affect phase dynamics on invariant tori $I_j = I$. Therefore we fix the normalization $C^2 = N/2$, where N is the number of oscillators, without loss of generality, to define an invariant torus $I_j = 1/2$. Due to the equivariance under scaling it is sufficient to study only one invariant torus. The dynamics is also invariant with respect to a global phase shift, because Eq. (2.5) depend only on the phase differences.

Involution (2.7) is valid in whole phase space of system (2.5), while the Hamiltonicity appears to be violated on invariant torus $I_j = 1/2$, since there are asymptotically stable trajectories on this manifold. We reason that one should take into account the behaviour of trajectories in vicinity of invariant torus to disclose that all attracting and repelling trajectories on it are actually saddle trajectories with zero sum of Lyapunov exponents. We will show by numerical procedures that this is actually the case. Thus all contractions and expansions of phase space on invariant torus are counterbalanced by expansions and contractions in its vicinity and phase volume is conserved. Nevertheless we regard the dynamics on ivariant torus $I_j = 1/2$ as degenerate. We point out an article [32] with similar situation. Bizyaev et al. show that the Hamiltonian problem of heavy rigid body motion (so-called Hess case) posess an invariant torus with limit cycles asimptotically stable at $t \to \infty$ or $t \to -\infty$. Interestingly, Bizyaev et al. reduced the problem at some special parameter values to Adler equation [36], describing a single phase oscillator. Another examples concern generalized Toda lattices, and also their connections to Chaplygin sleigh, Suslov problem and three-wave interaction [37].

Let us transform Eq. (2.5) with change of variables $I_j = a_j^2$ more suitable for numerical simulation, where $a_j > 0$ are real amplitudes of oscillations[2)]:

$$\begin{aligned}
\dot{a}_j =& -\varepsilon a_{j+1}\left(a_{j+1}^2 - a_j^2\right)\cos\left(\phi_{j+1}-\phi_j\right) - \varepsilon a_{j-1}\left(a_{j-1}^2 - a_j^2\right)\cos\left(\phi_{j-1}-\phi_j\right),\\
\dot{\phi}_j =& \omega_j + \beta a_j^2 + \varepsilon\left\{3a_{j+1}a_j - \frac{a_{j+1}^3}{a_j}\right\}\sin\left(\phi_{j+1}-\phi_j\right) + \varepsilon\left\{3a_{j-1}a_j - \frac{a_{j-1}^3}{a_j}\right\}\sin\left(\phi_{j-1}-\phi_j\right).
\end{aligned} \tag{2.10}$$

---

1) We consider phase shifts $\phi_{j+1} - \phi_j = \psi_j$ as variables, that undergo transformation.

2) Variables (a_j, ϕ_j) are not canonical variables of Hamiltonian (2.4).

In the next sections we study numerically the dynamics of Hamiltonian lattice (2.5) on invariant torus $I_j = 1/2$ and in its vicinity. We choose relatively simple lattices composed of $N = 3$ and $N = 4$ oscillators and set $\beta = 0$ for simplicity. We also shortly discuss system (2.5) composed of $N = 2$ oscillators.

3. TWO COUPLED HAMILTONIAN OSCILLATORS

The system of $N = 2$ conservative oscillators (2.5) is completely integrable. The invariant manifold $I_1 = I_2 = 1/2$ reduces to a circle parametrized by the phase shift $\psi = \phi_2 - \phi_1$, governed by Adler equation (we set $\beta = 0$):

$$\dot{\psi} = 1 - 2\varepsilon \sin\psi. \tag{3.1}$$

Equation (3.1) has two equilibria if $|\varepsilon| > 1/2$. One of them is stable $\mathcal{O}$ ($\psi_o = \arcsin\frac{1}{2\varepsilon}$) with characteristic Lyapunov exponent $\lambda = -\sqrt{4\varepsilon^2 - 1}$, another is unstable $\mathcal{S}$ ($\psi_s = \pi - \arcsin\frac{1}{2\varepsilon}$) with characteristic Lyapunov exponent $\lambda = \sqrt{4\varepsilon^2 - 1}$. But in a phase space of Hamiltonian model they both are saddles connected by heteroclinic trajectories on invariant circle and outside of it [34] (see Fig. 1).

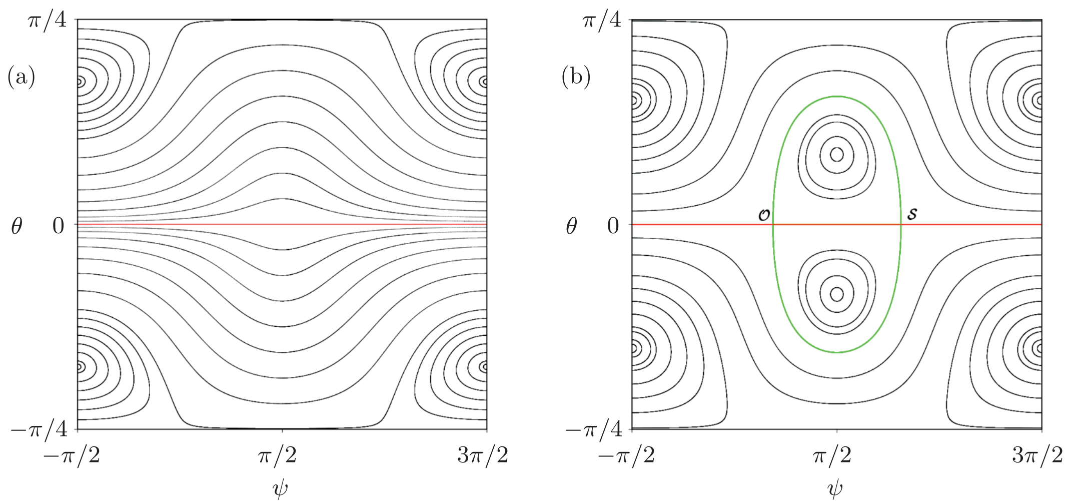

Fig. 1. (a) Phase portait of system (3.2) at $\varepsilon = 0.4$. (b) Phase portrait of system (3.2) at $\varepsilon = 0.9$. Saddle equilibria and their separatrices are marked on the figure.

We show that sums of characteristic Lyapunov exponents of equilibria $\mathcal{O}$ and $\mathcal{S}$ are zeroes in phase space of Hamiltonian model. First we take into account that phase space of Hamiltonian lattice is constrained by the equation $a_1^2 + a_2^2 = 1$ and by the fact that phases are defined up to arbitrary phase shift. Therefore we can reduce the system to two equations. We introduce new variable $\theta \in \left(-\frac{\pi}{4}, \frac{\pi}{4}\right)$ such that $\cos 2\theta = 2a_1a_2$, $\cos^2\theta = \frac{(a_1+a_2)^2}{2}$, $\sin^2\theta = \frac{(a_1-a_2)^2}{2}$:

$$\begin{aligned} \dot{\theta} &= \varepsilon \sin 2\theta \cos\psi, \\ \dot{\psi} &= 1 - 2\varepsilon \frac{\cos 4\theta}{\cos 2\theta} \sin\psi. \end{aligned} \tag{3.2}$$

The invariant circle is defined by value $\theta = 0$. We linearize Eq. (3.2) in the small neighborhood of $\mathcal{O}$ ($\theta_o = 0, \psi_o = \arcsin\frac{1}{2\varepsilon}$) and $\mathcal{S}$ ($\theta_s = 0, \psi_s = \pi - \arcsin\frac{1}{2\varepsilon}$):

$$\begin{aligned} \delta\dot{\theta} &= \pm\sqrt{4\varepsilon^2 - 1}\,\delta\theta, \\ \delta\dot{\psi} &= \mp\sqrt{4\varepsilon^2 - 1}\,\delta\psi. \end{aligned} \tag{3.3}$$

Therefore, equilibria $\mathcal{O}$ and $\mathcal{S}$ are saddles with Lyapunov exponents $\lambda_1 = \sqrt{4\varepsilon^2 - 1}$ and $\lambda_2 = -\sqrt{4\varepsilon^2 - 1}$ (the rest two exponents are zeroes due to constants of motion). Invariant circle $\theta = 0$ is stable manifold of $\mathcal{O}$ and unstable manifold of $\mathcal{S}$.

4. LATTICE OF $N = 3$ HAMILTONIAN OSCILLATORS

For lattices of $N = 3$ and $N = 4$ oscillators we submit the numerically calculated Lyapunov exponents for trajectories on invariant torus as well as illustrations of corresponding dynamics of phases on invariant torus and potential well populations in the vicinity of invariant torus. We investigated only trajectories symmetric by $\mathbf{R}$. We performed numerical integration of equations (2.5) using Dormand–Prince method with adaptive step implemented in Odeint library from Boost library collection [47]. Simulations were ran with check of constants of motions preservation up to numerical errors. We used well known Benettin procedure [3, 38, 39] for calculation of Lyapunov exponents with LAPACK subroutines for orthogonalization of perturbation vectors. According to Benettin algorithm we solved numerically Eq. (2.10) with $2N$ sets of variational equations. Each set of variational equations governed a perturbation vector. At constant timesteps we performed QR-decomposition of matrix composed of perturbation vectors. We accumulated sums of logarithms of diagonal elements of upper triangonal matrix R. These sums divided by integration time gave the estimations of Lyapunov exponents.

Figure 2 shows plots of Lyapunov exponents vs. ε of tipical trajectory on invariant torus (a) and of tipical trajectory, that does not belong to invariant torus (b), for lattice of $N = 3$ oscillators (other parameters are: $\beta = 0$, $\omega_1 = -1$, $\omega_2 = 0$, $\omega_3 = 1$). Picture (a) also contains plots of Lyapunov exponents for phase lattice (1.1) of Topaj and Pikovsky (red color in online version). Lyapunov exponents of phase model (1.1) match perfectly with half of the Lyapunov exponents of Hamiltonian model (2.5), that correspond to perturbation vectors always tangent to invariant torus $I_1 = I_2 = I_3 = 1/2$. At $|\varepsilon| < 1$ all Lyapunov exponents of trajectories on invariant torus are zero. This corresponds to periodic orbits on invariant torus [5]. At $|\varepsilon| > 1$ only two Lyapunov exponents are zero (since system (2.5) has two constants of motion), and other four are two pairs of positive and negative exponents. This corresponds to two saddle equilibriums in involution on invariant torus. On Fig. 2b only two Lyapunov exponents are zero at large ε. These Lyapunov exponents correspond to periodic saddle trajectories (Fig. 4b). The explanation is that symmetry induced by involution allows only periodic trajectories to cross Fix$\mathbf{R}$. This restriction takes place only in lattice of $N = 3$ oscillators.

Figure 3 demonstrates phase portraits of system (2.5) composed of $N = 3$ oscillators at $\varepsilon = 0.39$. All trajectories are symmetric, i. e. they cross the invariant set of involution Fix$\mathbf{R}$. Panel (a) shows trajectories belonging to invariant manifold $I_1 = I_2 = I_3 = 1/2$. It is a family of periodic orbits on invariant torus. Phase portrait is clearly symmetric with respect to $\mathbf{R}$. Figures 2b–2d show different projections of phase space for lattice with unfixed populations $I_1 = I_3 = 1/2 + 0.01$, $I_2 = 1/2 - 0.02$ (total population is $C^2 = 3/2$). If phase shifts $\phi_2 - \phi_1$ and $\phi_3 - \phi_2$ are close to $\pi/2$, populations deviate greatly from uniform distribution. Dynamics of phases on panel (b) is just slightly perturbed in comparison with dynamics on invariant torus (a).

At $\varepsilon = 1$ trajectories on the two-dimensional invariant torus $I_1 = I_2 = I_3 = 1/2$ condense at $\phi_2 - \phi_1 = \phi_3 - \phi_2 = \pi/2$. At $\varepsilon > 1$ stable equilibrium $\mathcal{O}_1 = \left(\arcsin\frac{1}{\varepsilon}, \arcsin\frac{1}{\varepsilon}\right)$ and unstable equilibrium $\mathcal{O}_2 = \left(\pi - \arcsin\frac{1}{\varepsilon}, \pi - \arcsin\frac{1}{\varepsilon}\right)$ appear which are effectively an attractor and a repeller of phase model (1.3) acting on the invariant torus $I_1 = I_2 = I_3 = 1/2$ of Eq. (2.5) (see Fig. 4a). These two points are in involution with each other so we can investigate only one of them. It is easy to find characteristic Lyapunov exponents of these equilibria by stability analysis of Eq. (1.3): $\mathcal{O}_1$ has both negative exponents $\lambda_1 = -\sqrt{\varepsilon^2 - 1}$ and $\lambda_2 = -3\sqrt{\varepsilon^2 - 1}$, $\mathcal{O}_2$ has both positive exponents $\lambda_1 = 3\sqrt{\varepsilon^2 - 1}$ and $\lambda_2 = \sqrt{\varepsilon^2 - 1}$. The dependencies of Lyapunov exponents correspond to Fig. 2a. Also together with equilibria $\mathcal{O}_{1,2}$ two saddle equilibria appear, which belong to Fix$\mathbf{R}$: $\mathcal{S}_1 = \left(\arcsin\frac{1}{\varepsilon}, \pi - \arcsin\frac{1}{\varepsilon}\right)$ and $\mathcal{S}_2 = \left(\pi - \arcsin\frac{1}{\varepsilon}, \arcsin\frac{1}{\varepsilon}\right)$. Both saddles have characteristic Lyapunov exponents with zero sum: $\lambda_1 = \sqrt{3(\varepsilon^2 - 1)}$ and $\lambda_2 = -\sqrt{3(\varepsilon^2 - 1)}$. Now we discuss stability of equilibria $\mathcal{O}_{1,2}$ and $\mathcal{S}_{1,2}$ in four-dimensional phase space of Hamiltonian model (we fixed $\mathcal{H} = 0$ and $C^2 = 3/2$). Every equilibrium on the invariant torus is a saddle with zero sum of Lyapunov exponents in phase space of Hamiltonian model. Saddle equilibria $\mathcal{O}_{1,2}$ have four nonzero Lyapunov exponents $\lambda_1 = 3\sqrt{\varepsilon^2 - 1}$, $\lambda_2 = \sqrt{\varepsilon^2 - 1}$, $\lambda_3 = -\sqrt{\varepsilon^2 - 1}$ and $\lambda_4 = -3\sqrt{\varepsilon^2 - 1}$. The invariant torus $I_1 = I_2 = I_3 = 1/2$ at $\varepsilon > 1$ is actually a stable manifold of saddle equilibrium $\mathcal{O}_1$ and unstable manifold of saddle equilibrium $\mathcal{O}_2$ in four-dimensional phase space.

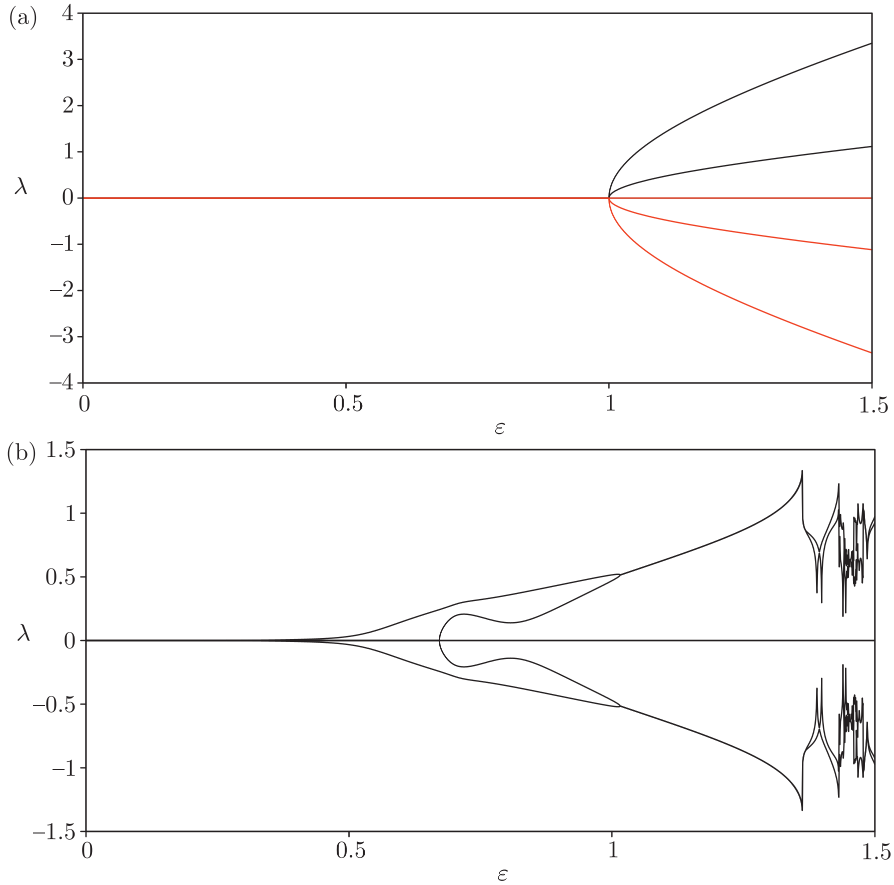

Fig. 2. (a) Plot of Lyapunov exponents vs. coupling parameter ε for lattice $N = 3$ of tipical trajectory on invariant torus (with initial condition $I_1 = I_2 = I_3 = 1/2$, $\phi_1 = \pi/3$, $\phi_2 = \pi/2$, $\phi_3 = 4\pi/3$). Lyapunov exponents of Topaj and Pikovsky phase lattice (1.1) are plotted red (see color online). (b) Plot of Lyapunov exponents vs. ε for tipical trajectory of the lattice $N = 3$ that does not belong to invariant torus (with initial conditions $I_1 = I_3 = 0.501$, $I_2 = 0.498$, such that constant C^2 is 3/2, $\phi_1 = \pi/3$, $\phi_2 = \pi/2$, $\phi_3 = 4\pi/3$). Other parameters are $\beta = 0$, $\omega_1 = -1$, $\omega_2 = 0$ and $\omega_3 = 1$.

5. LATTICE OF $N = 4$ HAMILTONIAN OSCILLATORS

Figure 5a demonstrates dependence on ε of Lyapunov exponents of Hamiltonian model (2.5) composed of $N = 4$ oscillators for trajectories on invariant torus $I_j = 1/2$. There are eight Lyapunov exponents, but four of them are always zero, two due to constants of motion and two due to invariance to arbitrary time shift along the trajectory and to arbitrary phase shift. Additionally the Lyapunov exponents for phase model (1.1) are plotted red (see color online). They coincide with four of eight exponents of Hamiltonian model (2.5) and describe only dynamics of phases on invariant torus. We distinguish four regions of ε. The first corresponds to quasiperiodic motions with all exponents equal to zero up to numerical errors ($\varepsilon < 0.38$ approximately). The second region ($\varepsilon < 0.43$ according to [5]) corresponds to coexistence of quasiperiodic and chaotic motions with one positive and one negative exponent (which appear to be equal in magnitude by our numerical approach) for perturbations tangent to the invariant torus (compare with exponents for phase lattice model (1.1)) and one positive and one negative exponent (equal in magnitude) for perturbations transversal to the invariant torus. The third region ($\varepsilon < 0.6$) is the interval[3] with coexisting "attractors" $\mathcal{A}$ and their reversal "repellers" $\mathcal{R}$ with one positive and one negative exponent for perturbations tangent to the invariant torus, nonequal in magnitude. Positive and negative exponents for perturbations transversal to the invariant torus are correspondingly equal

[3] Parameter ranges specified by us are not accurate, actually some small amount of trajectories might be asymptotic even if ε is close to zero [6].

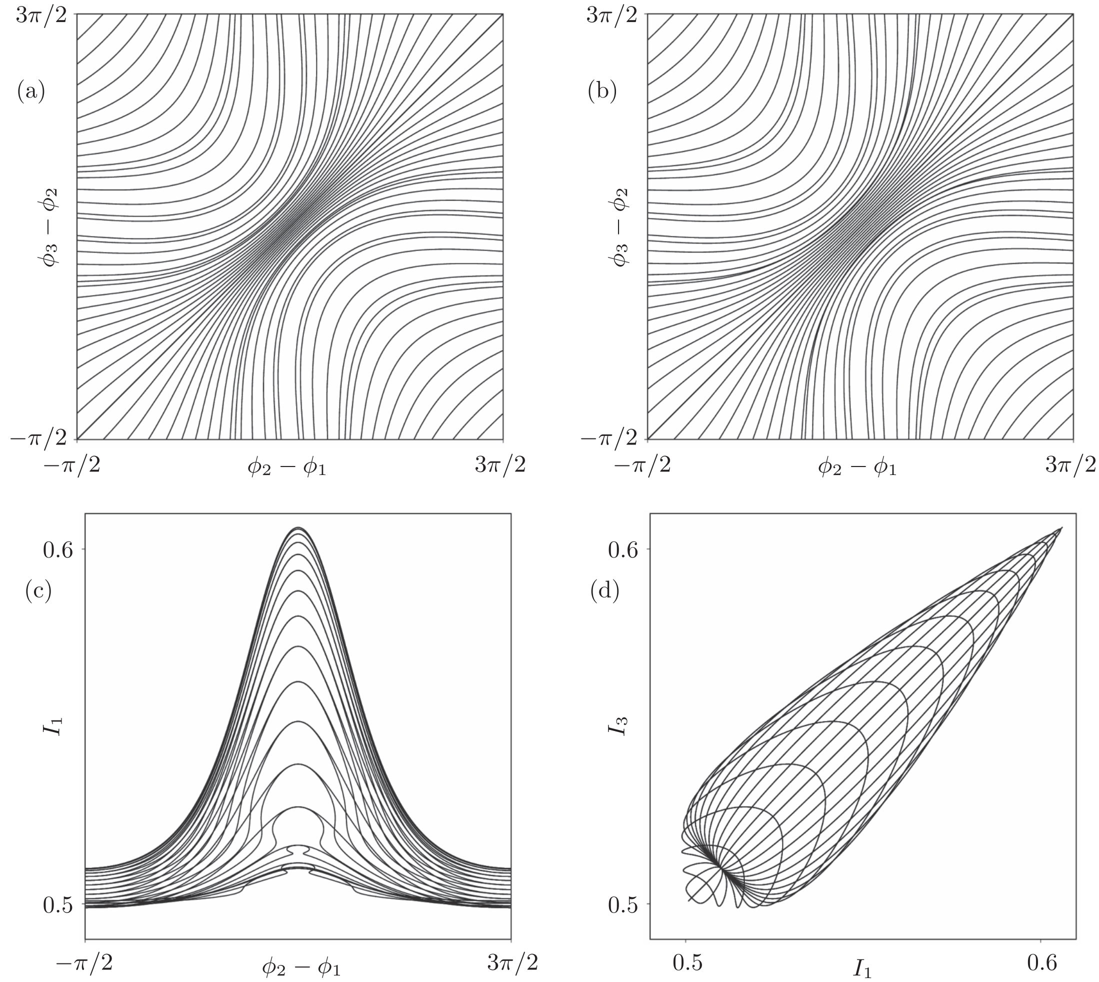

Fig. 3. Phase portraits of system (2.5) composed of $N = 3$ oscillators at parameter values $\beta = 0$, $\varepsilon = 0.39$, $\omega_1 = -1$, $\omega_2 = 0$, $\omega_3 = 1$. (a) Phase portrait for fixed populations $I_1 = I_2 = I_3 = 1/2$ and initial phases for all trajectories $\phi_2 - \phi_1 = \pi - (\phi_3 - \phi_2)$. (b,c,d) Phase portraits for unfixed populations $I_1 = I_3 = 1/2 + 0.01$, $I_2 = 1/2 - 0.02$, $\phi_2 - \phi_1 = \pi - (\phi_3 - \phi_2)$, panel (b) shows dynamics of phase shifts, (c) illustrates dynamics of population of first oscillator vs. phase shift between first and second oscillators, (d) shows evolution of populations of first and third oscillators.

in magnitude to negative and positive exponents for perturbations tangent to the invariant torus. Sets $\mathcal{A}$ attract only trajectories that belong to invariant torus and are actually saddle sets with zero sum of Lyapunov exponents. Behaviour of sets $\mathcal{R}$ is opposite. For roughly $\varepsilon > 0.6$ there are only periodic trajectories $\mathcal{C}_1$ and $\mathcal{C}_2$. Periodic orbit $\mathcal{C}_1$ has two nonequal negative Lyapunov exponents for perturbations tangent to the invariant torus, and two nonequal positive Lyapunov exponents for perturbations transversal to the invariant torus. Periodic orbit $\mathcal{C}_2$ is in involution with $\mathcal{C}_1$. In eight-dimensional phase space of Hamiltonian system both $\mathcal{C}_1$ and $\mathcal{C}_2$ are saddles with zero sums of Lyapunov exponents, but on four-dimensional invariant torus curve $\mathcal{C}_1$ acts like attractive limit cycle, and curve $\mathcal{C}_2$ acts like repelling limit cycle. Figure 5b shows plots of panel (a) enlarged. One can see, that symmetry of Topaj and Pikovsky phase lattice is broken at large values of ε, while Hamiltonian model has nonzero Lyapunov exponents split and anomaly of phase dynamics compensated by behaviour of populations I_j.

To visualize dynamics of system (2.5) with $N = 4$ oscillators we need to construct suitable Poincaré cross-section. We follow [5] and choose cross-section by surface $\phi_3 - \phi_2 = \pi/2$ so that the invariant set of the involution is $\phi_2 - \phi_1 = \pi - (\phi_4 - \phi_3)$, $I_1 = I_4$, $I_2 = I_3$ on this surface[4)].

[4)] We should note, that some trajectories are tangent to this cross-section surface. See another set of phase variables in [6, 12], that does not have this disadvantage.

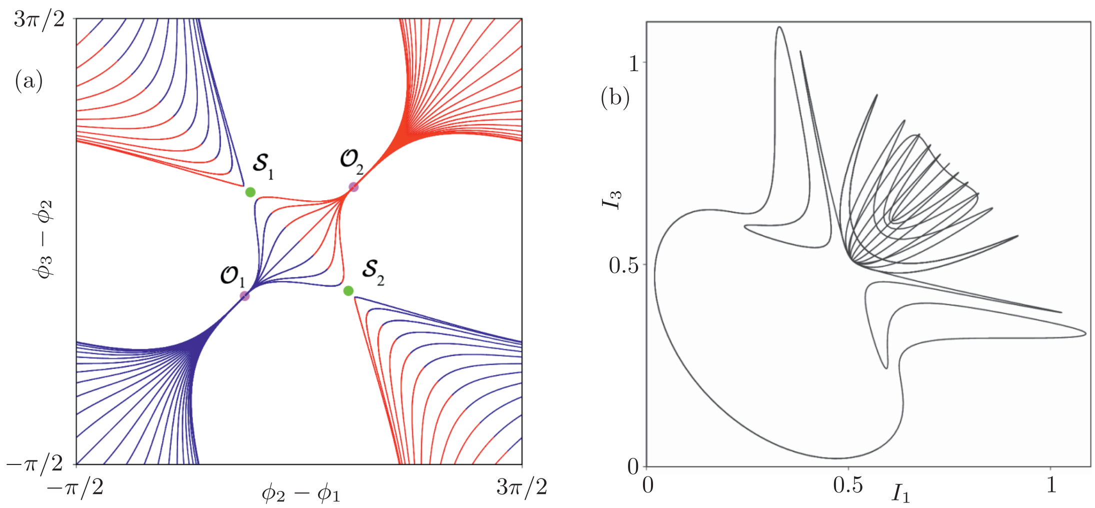

Fig. 4. Phase portraits of system (2.5) composed of $N = 3$ oscillators at parameter values $\beta = 0$, $\varepsilon = 1.39$, $\omega_1 = -1$, $\omega_2 = 0$, $\omega_3 = 1$. (a) Phase portrait for fixed populations $I_1 = I_2 = I_3 = 1/2$ and initial phases for all trajectories $\phi_2 - \phi_1 = \pi - (\phi_3 - \phi_2)$. Trajectories approaching equilibria $\mathcal{O}_1$ at $t \to \infty$ are plotted blue, trajectories approaching equilibria $\mathcal{O}_2$ at $t \to -\infty$ are plotted red (color online). (b) An example of symmetric trajectories that do not belong to invariant torus. Initial conditions are $I_1 = I_3 = 1/2 + 0.01$, $I_2 = 1/2 - 0.02$, $\phi_2 - \phi_1 = \pi - (\phi_3 - \phi_2)$.

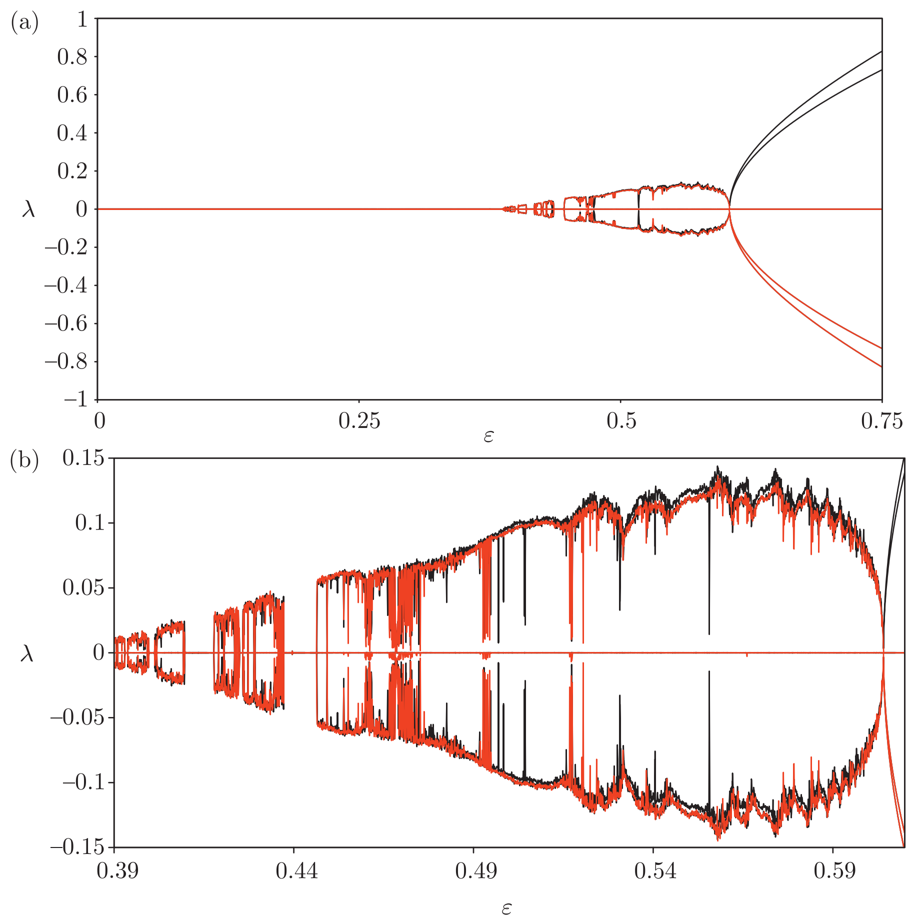

Fig. 5. (a) Plot of Lyapunov exponents vs. coupling parameter ε for lattice $N = 4$ of tipical trajectory on invariant torus (with initial condition $I_1 = I_2 = I_3 = I_4 = 1/2$, $\phi_1 = -\pi/2$, $\phi_2 = 4\pi/3$, $\phi_3 = -\pi/6$, $\phi_4 = \pi$). Lyapunov exponents of Topaj and Pikovsky phase lattice (1.1) are plotted red (color online). (b) Enlarged part of panel (a). Overlap of Lyapunov exponents of models (1.1) and (2.5), corresponding to perturbations tangent to invariant manifold, is clear. Other parameters are $\beta = 0$, $\omega_1 = -1.5$, $\omega_2 = -0.5$, $\omega_3 = 0.5$ and $\omega_4 = 1.5$.

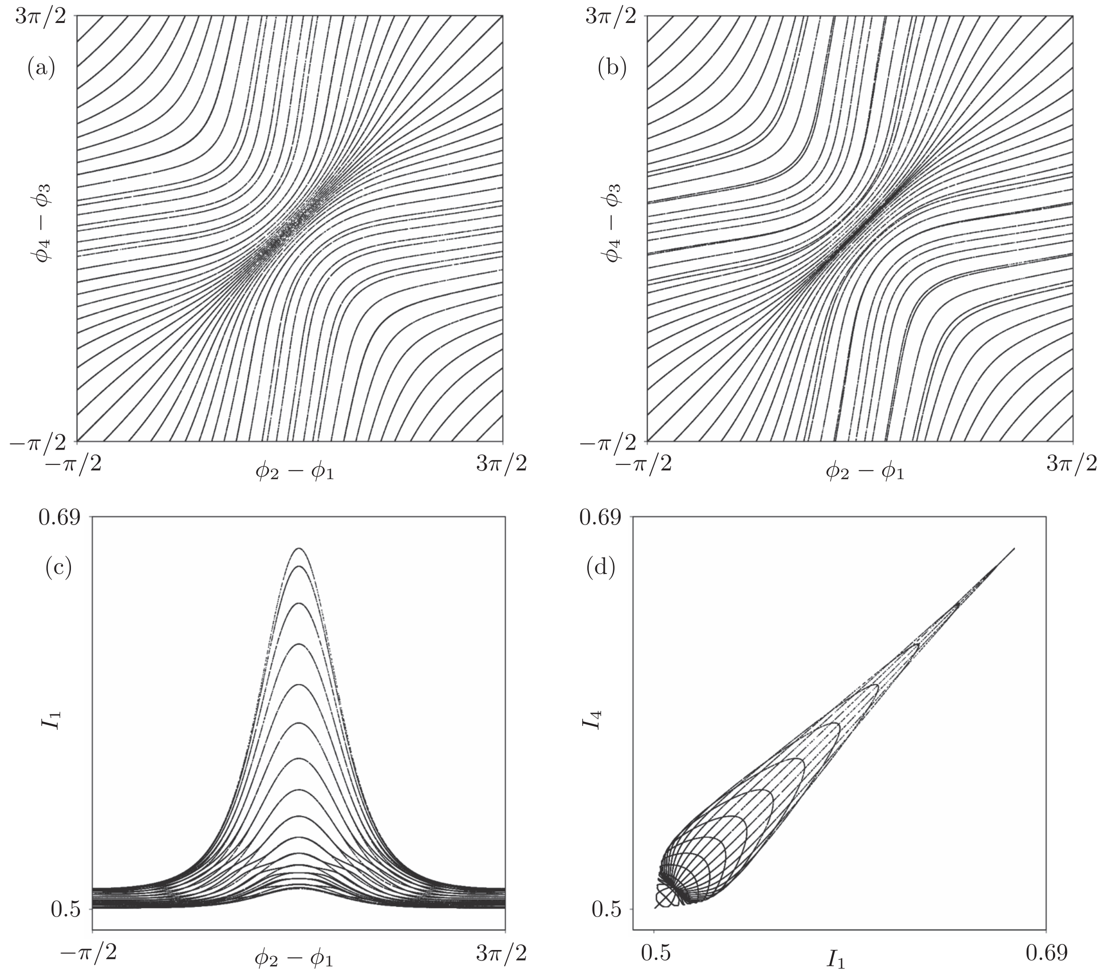

Fig. 6. Phase portraits of system (2.5) composed of $N = 4$ oscillators in Poincaré cross-section at parameter values $\beta = 0$, $\varepsilon = 0.19$, $\omega_1 = -1.5$, $\omega_2 = -0.5$, $\omega_3 = 0.5$, $\omega_4 = 1.5$ (quasiperiodic regimes). (a) Phase portrait for fixed populations $I_1 = I_2 = I_3 = I_4 = 1/2$ and initial phases for all trajectories $\phi_2 - \phi_1 = \pi - (\phi_4 - \phi_3)$, $\phi_3 - \phi_2 = \pi/2$. (b,c,d) Phase portraits for unfixed populations $I_1 = I_4 = 1/2 + 0.01$, $I_2 = I_3 = 1/2 - 0.01$, $\phi_2 - \phi_1 = \pi - (\phi_4 - \phi_3)$, $\phi_3 - \phi_2 = \pi/2$, panel (b) shows dynamics of phase shifts, (c) illustrates dynamics of population of first oscillator vs. phase shift between first and second oscillators, (d) shows evolution of populations of first and last oscillators.

Figure 6 shows phase portraits of Poincaré map of the system (2.5) composed of $N = 4$ oscillators at $\varepsilon = 0.19$. All trajectories are symmetric. Panel (a) shows trajectories belonging to invariant manifold $I_1 = I_2 = I_3 = I_4 = 1/2$. It is a family of quasiperiodic trajectories (invariant curves) on invariant torus. Phase portrait is clearly symmetric with respect to $\mathbf{R}$. Figures 6b–6d show different projections of phase space for lattice with unfixed populations $I_1 = I_4 = 1/2 + 0.01$, $I_2 = I_3 = 1/2 - 0.01$ (total population is $C^2 = 2$). We describe motions in the neigborhood of the invariant torus following paper [34]. If phase shifts $\phi_2 - \phi_1$ and $\phi_4 - \phi_3$ between neiboring oscillators become close to $\pi/2$, their populations unlock from uniform distribution $I_j \approx 1/2$, grow fast and then return. We conclude that populations I_j oscillate near invariant torus if initially distributed close to $I = 1/2$. Dynamics of phases in case of almost uniform dustribution of I_j is very close to dynamics on the invariant torus.

Figure 7 demonstrates phase portraits in Poincaré cross-section of the system (2.5) with $N = 4$ oscillators at $\varepsilon = 0.39$. Panel (a) shows trajectories on invariant torus. It is a “sea” of chaotic trajectories with “islands” of quasiperiodic and periodic motions, like in nonintegrable Hamiltonian systems. It is possible, however, that some of the trajectories on invariant torus asymptotically converge [6]. As before, we state that asymptotically stable trajectories on invariant torus are unstable in transversal directions with rates of convergence and divergence balanced. Figures 7b–

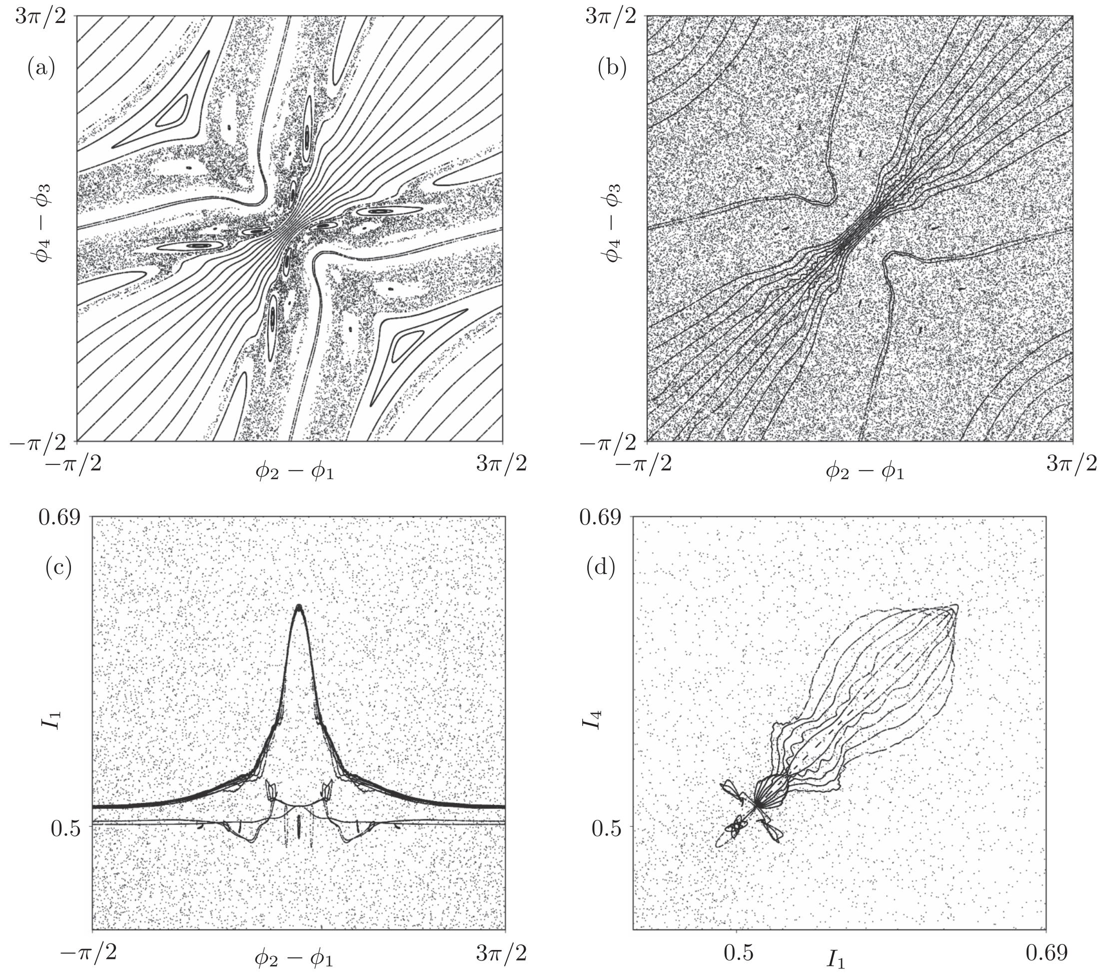

Fig. 7. Phase portraits of system (2.5) composed of $N = 4$ oscillators in Poincaré cross-section at parameter values $\beta = 0$, $\varepsilon = 0.39$, $\omega_1 = -1.5$, $\omega_2 = -0.5$, $\omega_3 = 0.5$, $\omega_4 = 1.5$ ("chaotic sea"). (a) Phase portrait for fixed populations $I_1 = I_2 = I_3 = I_4 = 1/2$ and initial phases for all trajectories $\phi_2 - \phi_1 = \pi - (\phi_4 - \phi_3)$, $\phi_3 - \phi_2 = \pi/2$. (b,c,d) Phase portraits for unfixed populations $I_1 = I_4 = 1/2 + 0.01$, $I_2 = I_3 = 1/2 - 0.01$, $\phi_2 - \phi_1 = \pi - (\phi_4 - \phi_3)$, $\phi_3 - \phi_2 = \pi/2$, panel (b) shows dynamics of phase shifts, (c) illustrates dynamics of population of first oscillator vs. phase shift between first and second oscillators, (d) shows evolution of populations of first and last oscillators.

7d show projections of phase space for lattice with unfixed populations. One can see, that chaotic layers are not bounded by KAM-tori. This is a well-known Arnol'd diffusion phenomenon [40].

Figure 8 demonstrates Poincaré cross-section at $\varepsilon = 0.49$. Panel (a) and panel (b) show evolution of trajectories on invariant torus starting from Fix$\mathbf{R}$ forward and backward in time. Symmetric trajectories converge to "attracting" set $\mathcal{A}$ at $t \to \infty$ and to "repelling" set $\mathcal{R}$ at $t \to -\infty$. Sets $\mathcal{A}$ and $\mathcal{R}$ do not coincide with each other, but are in involution. This is an example of symmetry breaking in phase lattice model of Pikovsky and Topaj. Again we emphasize, that $\mathcal{A}$ and $\mathcal{R}$ are saddle sets in a phase space of Hamiltonian system (2.5) with equal rates of divergence and convergence. We do not submit portraits of trajectories in vicinity of invariant torus, because KAM-tori are almost absent and it is impossible to distinguish any pattern due to Arnol'd diffusion.

6. CONCLUSION

We studied the Hamiltonian generalization of Pikovsky and Topaj reversible lattice of locally coupled phase oscillators. The Hamiltonian model has the involution similar to the one in Topaj–Pikovsky lattice. Furthermore the Hamiltonian system has invariant manifolds where dynamics reduces precisely to the phase model of Pikovsky and Topaj. We showed that asymptotic behavior on these manifolds did not contradict to overall conservativity of Hamiltonian system. We considered

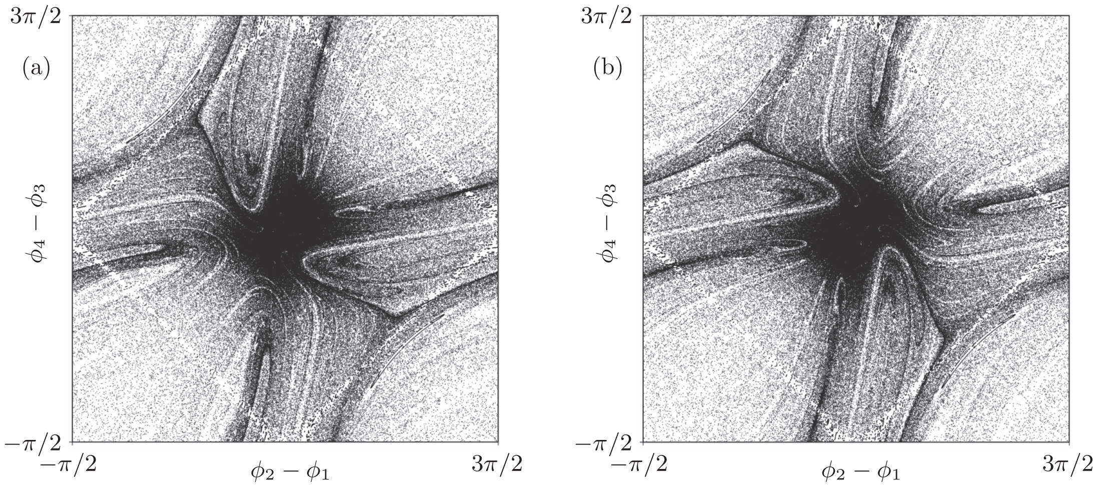

Fig. 8. Phase portraits of system (2.5) composed of $N = 4$ oscillators in Poincaré cross-section at parameter values $\beta = 0$, $\varepsilon = 0.49$, $\omega_1 = -1.5$, $\omega_2 = -0.5$, $\omega_3 = 0.5$, $\omega_4 = 1.5$ (chaotic "attractor" and "repeller"). Initial conditions are $I_1 = I_2 = I_3 = I_4 = 1/2$, $\phi_2 - \phi_1 = \pi - (\phi_4 - \phi_3)$, $\phi_3 - \phi_2 = \pi/2$. (a) Evolution forward in time. (b) Evolution backward in time.

three simple examples of the Hamiltonian lattice. In case of only two coupled oscillators the invariant manifold reduces to a circle. At large values of coupling parameter two saddles emerge on the invariant circle, and the invariant circle becomes composed of their separatrices. If one consider the dynamics only on the invariant circle, it looks dissipative, but in a whole phase space the volume preserves. In case of lattices of three or four oscillators the situation is similar. The invariant manifolds are tori and at large coupling parameter they hold saddle trajectories. If, again, one consider only the dynamics on invariant tori, it looks non-conservative, but actually the contrary. All saddle trajectories that belong to the invariant tori, have stable and unstable manifolds with equal convergence and divergence rates, and do not violate the conservation of phase volume. Starting from $N = 4$ oscillators the lattice manifests very complex dynamics. We also slightly covered the dynamics of symmetric by involution trajectories that do not belong to invariant manifolds. In lattices of two and three oscillators symmetric trajectories appear to be only periodic (in case of $N = 3$ we have a numerical evidence), because they have to map into themselves by involution and the dimension of phase spase is not big enough to allow more complex symmetric trajectories. In lattice of four oscillators we observed not only chaotic trajectories, but also Arnol'd diffusion in vicinity on invariant manifolds. Overall the Topaj – Pikovsky reversible (but not conservative) lattice can be considered as a special case of Hamiltonian lattice introduced in [33]. At the same time we suppose that it is still fair to consider Topaj – Pikovsky phase lattice as an independent problem.

In our research we followed [34]. We believe this new approach to generalize ansambles of phase oscillators up to Hamiltonian systems will pay off in future studies. For example it may bring a fresh look on a famous Watanage–Strogatz partial integrability in ansamble of globally coupled identical Kuramoto oscillators [41–45]. At last we want to point out the article [46] exploring the connection between synchronization and quantum entanglement by introduction of quantized version of Hamiltonian model from [34].

ACKNOWLEDGMENTS

The authors thank Prof. A. V. Borisov, who inspired them to research the Topaj – Pikovsky problem and its possible generalizations. The authors thank A. R. Safin for bringing article [34] to their attention. The authors thank A. Pikovsky, L. A. Smirnov, I. R. Sataev and A. O. Kazakov for useful discussions.

FUNDING

The work of V. P. Kruglov and S. P. Kuznetsov was supported by the grant of the Russian Science Foundation (project no. 15-12-20035) in part of formulation of the problem, analytical calculations and research of related topics (Sections 1 and 2). The work of V. P. Kruglov was supported by the grant of the Russian Science Foundation (project no. 19-71-30012) in part of analitical and numerical calculations and interpretation of obtained results (Sections 3–6).

CONFLICT OF INTEREST

The authors declare that they have no conflicts of interest.

REFERENCES

1. Kuramoto, Y., *Chemical Oscillations, Waves, and Turbulence,* Springer Ser. Synergetics, vol. 19, Berlin: Springer, 1984.
2. Pikovsky, A., Rosenblum, M., and Kurths, J., *Synchronization: A Universal Concept in Nonlinear Sciences,* Cambridge Nonlinear Sci. Ser., vol. 12, New York: Cambridge Univ. Press, 2001.
3. Pikovsky, A. and Politi, A., *Lyapunov Exponents: A Tool to Explore Complex Dynamics,* Cambridge: Cambridge Univ. Press, 2016.
4. Strogatz, S. H., From Kuramoto to Crawford: Exploring the Onset of Synchronization in Populations of Coupled Oscillators. Bifurcations, Patterns and Symmetry, *Phys. D,* 2000, vol. 143, nos. 1–4, pp. 1–20.
5. Topaj, D. and Pikovsky, A., Reversibility vs. Synchronization in Oscillator Lattices, *Phys. D,* 2002, vol. 170, no. 2, pp. 118–130.
6. Gonchenko, A. S., Gonchenko, S. V., Kazakov, A. O., and Turaev, D. V., On the Phenomenon of Mixed Dynamics in Pikovsky – Topaj System of Coupled Rotators, *Phys. D,* 2017, vol. 350, pp. 45–57.
7. Kuznetsov, A. P., Rahmanova, A. Z., and Savin, A. V., The Effect of Symmetry Breaking on Reversible Systems with Mixed Dynamics, *Izv. Vyssh. Uchebn. Zaved. Prikl. Nelin. Dinam.,* 2018, vol. 26, no. 6, pp. 20–31 (Russian).
8. Tsang, K. Y., Mirollo, R. E., Strogatz, S. H., and Wiesenfeld, K., Reversibility and Noise Sensitivity of Josephson Arrays, *Phys. Rev. Lett.,* 1991, vol. 66, no. 8, pp. 1094–1097.
9. Roberts, J. A. G. and Quispel, G. R. W., Chaos and Time-Reversal Symmetry. Order and Chaos in Reversible Dynamical Systems, *Phys. Rep.,* 1992, vol. 216, nos. 2–3, pp. 63–177.
10. Lamb, J. S. W. and Roberts, J. A. G., Time-Reversal Symmetry in Dynamical Systems: A Survey, *Phys. D,* 1998, vol. 112, nos. 1–2, pp. 1–39.
11. Lerman, L. M. and Turaev, D. V., Breakdown of Symmetry in Reversible Systems, *Regul. Chaotic Dyn.,* 2012, vol. 17, nos. 3–4, pp. 318–336.
12. Delshams, A., Gonchenko, S. V., Gonchenko, A. S., Lázaro, J. T., and Sten'kin, O., Abundance of Attracting, Repelling and Elliptic Periodic Orbits in Two-Dimensional Reversible Maps, *Nonlinearity,* 2013, vol. 26, no. 1, pp. 1–33.
13. Moser, J. K. and Webster, S. M., Normal Forms for Real Surfaces in C^2 near Complex Tangents and Hyperbolic Surface Transformations, *Acta Math.,* 1983, vol. 150, no. 1, pp. 255–296.
14. Scheurle, J., Bifurcation of Quasi-Periodic Solutions from Equilibrium Points of Reversible Dynamical Systems, *Arch. Rational Mech. Anal.,* 1987, vol. 97, no. 2, pp. 103–139.
15. Bibikov, Yu. N. and Pliss, V. A., On the Existence of Invariant Tori in a Neighborhood of the Zero Solution of a System of Ordinary Differential Equations, *Differ. Equ.,* 1967, vol. 3, no. 11, pp. 967–976; see also: *Differ. Uravn.,* 1967, vol. 3, no. 11, pp. 1864–1881.
16. Lamb, J. S. W. and Stenkin, O. V., Newhouse Regions for Reversible Systems with Infinitely Many Stable, Unstable and Elliptic Periodic Orbits, *Nonlinearity,* 2004, vol. 17, no. 4, pp. 1217–1244.
17. Gonchenko, S. V. and Turaev, D. V., On Three Types of Dynamics and the Notion of Attractor, *Proc. Steklov Inst. Math.,* 2017, vol. 297, no. 1, pp. 116–137; see also: *Tr. Mat. Inst. Steklova,* 2017, vol. 297, pp. 133–157.
18. Politi, A., Oppo, G. L., and Badii, R., Coexistence of Conservative and Dissipative Behavior in Reversible Dynamical Systems, *Phys. Rev. A,* 1986, vol. 33, no. 6, pp. 4055–4060.
19. Gonchar, V. Yu., Ostapchuk, P. N., Tur, A. V., and Yanovsky, V. V., Dynamics and Stochasticity in a Reversible System Describing Interaction of Point Vortices with a Potential Wave, *Phys. Lett. A,* 1991, vol. 152, nos. 5–6, pp. 287–292.
20. Vetchanin, E. V. and Kazakov, A. O., Bifurcations and Chaos in the Dynamics of Two Point Vortices in an Acoustic Wave, *Internat. J. Bifur. Chaos Appl. Sci. Engrg.,* 2016, vol. 26, no. 4, 1650063, 13 pp.
21. Vetchanin, E. V. and Mamaev, I. S., Dynamics of Two Point Vortices in an External Compressible Shear Flow, *Regul. Chaotic Dyn.,* 2017, vol. 22, no. 8, pp. 893–908.
22. Borisov, A. V. and Mamaev, I. S., Strange Attractors in Rattleback Dynamics, *Physics-Uspekhi,* 2003, vol. 46, no. 4, pp. 393–403; see also: *Uspekhi Fiz. Nauk,* 2003, vol. 173, no. 4, pp. 407–418.

23. Borisov, A. V., Jalnine, A. Yu., Kuznetsov, S. P., Sataev, I. R., and Sedova, J. V., Dynamical Phenomena Occurring due to Phase Volume Compression in Nonholonomic Model of the Rattleback, *Regul. Chaotic Dyn.,* 2012, vol. 17, no. 6, pp. 512–532.
24. Gonchenko, A. S., Gonchenko, S. V., and Kazakov, A. O., Richness of Chaotic Dynamics in Nonholonomic Models of a Celtic Stone, *Regul. Chaotic Dyn.,* 2013, vol. 18, no. 5, pp. 521–538.
25. Borisov, A. V., Kazakov, A. O., and Kuznetsov, S. P., Nonlinear Dynamics of the Rattleback: A Nonholonomic Model, *Physics-Uspekhi,* 2014, vol. 57, no. 5, pp. 453–460; see also: *Uspekhi Fiz. Nauk,* 2014, vol. 184, no. 5, pp. 493–500.
26. Borisov, A. V., Kazakov, A. O., and Sataev, I. R., Spiral Chaos in the Nonholonomic Model of a Chaplygin Top, *Regul. Chaotic Dyn.,* 2016, vol. 21, nos. 7–8, pp. 939–954.
27. Bizyaev, I. A., Borisov, A. V., and Kazakov, A. O., Dynamics of the Suslov Problem in a Gravitational Field: Reversal and Strange Attractors, *Regul. Chaotic Dyn.,* 2015, vol. 20, no. 5, pp. 605–626.
28. Borisov, A. V., Kilin, A. A., and Mamaev, I. S., Hamiltonicity and Integrability of the Suslov Problem, *Regul. Chaotic Dyn.,* 2011, vol. 16, nos. 1–2, pp. 104–116.
29. Bolsinov, A. V., Borisov, A. V., and Mamaev, I. S., Hamiltonization of Non-Holonomic Systems in the Neighborhood of Invariant Manifolds, *Regul. Chaotic Dyn.,* 2011, vol. 16, no. 5, pp. 443–464.
30. Borisov, A. V., Mamaev, I. S., and Tsyganov, A. V., Nonholonomic Dynamics and Poisson Geometry, *Russian Math. Surveys,* 2014, vol. 69, no. 3, pp. 481–538; see also: *Uspekhi Mat. Nauk,* 2014, vol. 69, no. 3(417), pp. 87–144.
31. Bizyaev, I. A., Borisov, A. V., and Mamaev, I. S., Hamiltonization of Elementary Nonholonomic Systems, *Russ. J. Math. Phys.,* 2015, vol. 22, no. 4, pp. 444–453.
32. Bizyaev, I. A., Borisov, A. V., and Mamaev, I. S., The Hess – Appelrot Case and Quantization of the Rotation Number, *Regul. Chaotic Dyn.,* 2017, vol. 22, no. 2, pp. 180–196.
33. Thommen, Q., Garreau, J. C., and Zehnlé, V., Classical Chaos with Bose – Einstein Condensates in Tilted Optical Lattices, *Phys. Rev. Lett.,* 2003, vol. 91, no. 21, 210405, 4 pp.
34. Witthaut, D. and Timme, M., Kuramoto Dynamics in Hamiltonian Systems, *Phys. Rev. E,* 2014, vol. 90, no. 3, 032917, 8 pp.
35. Witthaut, D., Werder, M., Mossmann, S., and Korsch, H. J., Bloch Oscillations of Bose – Einstein Condensates: Breakdown and Revival, *Phys. Rev. E,* 2005, vol. 71, no. 3, 036625, 9 pp.
36. Adler, R., A Study of Locking Phenomena in Oscillators, *Proc. IRE,* 1946, vol. 34, no. 6, pp. 351–357.
37. Bloch, A. M., Asymptotic Hamiltonian Dynamics: The Toda Lattice, the Three-Wave Interaction and the Non-Holonomic Chaplygin Sleigh, *Phys. D,* 2000, vol. 141, nos. 3–4, pp. 297–315.
38. Benettin, G., Galgani, L., Giorgilli, A., and Strelcyn, J.-M., Lyapunov Characteristic Exponents for Smooth Dynamical Systems and for Hamiltonian Systems: A Method for Computing All of Them: P. 1: Theory, *Meccanica,* 1980, vol. 15, no. 1, pp. 9–20.
39. Shimada, I. and Nagashima, T., A Numerical Approach to Ergodic Problem of Dissipative Dynamical Systems, *Progr. Theoret. Phys.,* 1979, vol. 61, no. 6, pp. 1605–1616.
40. Arnol'd, V. I., Instability of Dynamical Systems with Many Degrees of Freedom, *Dokl. Akad. Nauk SSSR,* 1964, vol. 156, no. 1, pp. 9–12 (Russian).
41. Watanabe, Sh. and Strogatz, S. H., Integrability of a Globally Coupled Oscillator Array, *Phys. Rev. Lett.,* 1993, vol. 70, no. 16, pp. 2391–2394.
42. Watanabe, S. and Strogatz, S. H., Constants of Motion for Superconducting Josephson Arrays, *Phys. D,* 1994, vol. 74, nos. 3–4, pp. 197–253.
43. Marvel, S., Mirollo, R., and Strogatz, S., Identical Phase Oscillators with Global Sinusoidal Coupling Evolve by Möbius Group Action, *Chaos,* 2009, vol. 19, no. 4, 043104, 11 pp.
44. Vlasov, V., Rosenblum, M., and Pikovsky, A., Dynamics of Weakly Inhomogeneous Oscillator Populations: Perturbation Theory on Top of Watanabe – Strogatz Integrability, *J. Phys. A,* 2016, vol. 49, no. 31, 31LT02, 8 pp.
45. Lohe, M. A., Higher-Dimensional Generalizations of the Watanabe – Strogatz Transform for Vector Models of Synchronization, *J. Phys. A,* 2018, vol. 51, no. 22, 225101, 24 pp.
46. Witthaut, D., Wimberger, S., Burioni, R., and Timme, M., Classical Synchronization Indicates Persistent Entanglement in Isolated Quantum Systems, *Nat. Commun.,* 2017, vol. 8, Art. 14829, 7 pp.
47. Ahnert, K. and Mulansky, M., Odeint — Solving Ordinary Differential Equations in C++, *AIP Conf. Proc.,* 2011, vol. 1389, no. 1, pp. 1586–1589.